Experimental Demonstration of the Effectiveness of an Early Streamer Emission Air Terminal Versus a Franklin Rod

L. Pecastaing, T. Reess, A. De Ferron, S. Souakri
Laboratoire SIAME, Equipe Génie Electrique,
Université de Pau et des Pays de l'Adour,
Hélioparc Pau-Pyrénées, 2 av Angot 64053 Pau cedex 9, France

E. Smycz
Piorteh and Orw-Els companies, 53 rue Berthe, 75018 Paris, France

A. Skopec and **C. Stec**
Institute of the Fundamentals of Electrotechnics and Electrotechnology
Wroclaw University of Technology, Wybrzeze Wyspianskiego
27, 53-370, Wroclaw, Poland

ABSTRACT

This paper is devoted to a detailed presentation of all aspects involved in a novel experimental technique to prove the effectiveness of an early streamer emission air terminal (ESEAT) versus a traditional Franklin rod in a laboratory. Firstly, a theoretical basis for the equivalent-circuit analysis of an ESEAT model is presented. It is shown that the dynamic electric field intensity on the active ESE rod is higher (theoretically even twice as high) than the static field intensity of the conventional Franklin lightning rod. Then, an experimental test using a method and associated with an electrostatic simulation demonstrates the effectiveness of an ESEAT (Pix3-60 from Piorteh Company) versus a conventional Franklin rod in the SIAME laboratory of the University of Pau in France. This method consists in locating both the ESE terminal and the Franklin rod together in the same configuration in accordance with the French Standard NFC 17-102 (09/2011). During the tests, all discharges were recorded on the ESEAT manufactured by Piorteh Company when its rod was active. This experimental test could be used on any kind of lightning protection device.

Index Terms - **Lightning protection, early streamer emission, electrical discharge, effectiveness evaluation, active rods.**

1 INTRODUCTION

THE investigation of atmospheric discharges belongs to the most complex challenges of science and technology, requiring a broad interdisciplinary approach. This is due to the fact that an extremely large number of factors in a cause and effect relationship are involved in the generation and development of atmospheric electricity phenomena, particularly the accumulation of an electric charge and the various forms of its discharge. It is only known that the lightning protection devices are studied and for the last decade or so increasingly employed.

The effectiveness of the standard Franklin rod, used in lightning protection, is known to depend on the development of a corona effect near its tip as the result of high electric fields developed in a lightning storm [1]. With the approach of a downward leader, the resulting rapid field enhancement increases corona activity. When electrical conditions are fulfilled, one of the streamer filaments which constitute the corona may undergo sufficient heating to develop into a highly conductive, arc-like 'upward leader' which can then propagate for a considerable distance in a comparatively low electric field. It may thus progress towards the downward leader. The downward and upward leader will meet thus forming one new leader bridging the gap and allow the subsequent high-current discharge to pass down the conducting path so formed.

A simple passive Franklin rod, on the roof of a large building, may not give full protection against a strike to the building itself, since upward corona may be initiated at parts of the structure more favorably placed in relation to the downward leader. A much better efficiency can be expected however from an 'active' rod, for which a corona effect is initiated at an early time during the downward progress of the lightning.

Manuscript received on 3 March 2014, in final form 4 November 2014, accepted 13 November 2014.

DOI 10.1109/TDEI.2014.004629

This principle forms the basis of the so-called early streamer emission devices which have been developed in recent years. The success of such a device depends on the timing of the corona initiation in relation to the downward leader approach and the rapidity with which the leaders can attach compared with the time that would have been taken with passive rods. During the lightning in negative polarity, the propagation of a negative downward leader systematically leads to the development of a positive upward leader [2]. The development of this upward leader is conditioned by the electric field increase induced by the downward leader near an asperity (e.g. lightning protection device). In the case of an ESEAT, the positive corona or upward leader is initiated by the active lightning protection device regardless of the position of the downward leader. The breakdown time is therefore decreased.

Three types of lightning protection systems are in common use today: conventional systems, Charge Transfer Systems, and systems based on Early Streamer Emission air terminals (ESEAT) [3].The purpose of a lightning protection system (LPS) is to prevent or greatly reduce damage from a direct or nearby lightning strike to the protected facility. A conventional LPS is designed to prevent damage by providing a number of preferential strike receptors (air terminals) with low impedance paths to conduct the large lightning current harmlessly to the ground. ESEAT are claimed to have a much larger zone of protection than conventional lightning air terminals, resulting in an LPS with significantly fewer air terminals and down conductors than a conventional one. Studies have shown that taking into account the upward leader increases the radius of the protection sphere in the electrogeometric model [4].

There are a few types of ESEAT working on a different principle [5]:

- The air ionization at the tip is produced by piezoelectric element using the wind energy,
- The air ionization is caused by electrical impulses delivered by a generator. The electrical field of downward leader charges a capacitor which supplies the generator,
- The high voltage impulse is induced by the electromagnetic impulse in a coil. The product presented in this paper (Pix3-60 manufactured by Piorteh Company) is based upon this principle. Here a theoretical basis of active rod is presented at first and then an experimental test using a novel method and associating with an electrostatic simulation demonstrates its effectiveness versus a conventional Franklin rod in a laboratory.

2 TEST TECHNIQUES OF LIGHTNING PROTECTION SYSTEMS

Because of the considerable danger to life and property arising from lightning discharges, lightning protection improvement constitutes an important technical and economic issue. Since 100% lightning protection is technically and economically impossible, it is essential to seek and use protective devices substantially increasing its effectiveness. Active ESEAT meet such requirements. Nevertheless the current opinions about active rods are often controversial and contradictory [5-9]. Various experiments are presented in laboratory or in nature under operating conditions. The effectiveness of ESEAT is clearly demonstrated in laboratory conditions. However, under natural conditions, their effectiveness is difficult to prove and is not unanimous.

In order to discuss the LPS technology, it is necessary to have a basic understanding of the phenomenology of the lightning process. More detailed discussion can be found in standard references on lightning (e.g., [10]). The electric fields on the ground under a thunderstorm are typically 5 to 20 kV/m [3]. The field at the tip of an exposed lightning conductor terminal can thus be expected to be much higher. These conditions can be simulated in the laboratory by application of a DC voltage to a large object suspended above a conductor. The subsequent descent of the leader is simulated by the super-imposition of an impulse voltage to the gap, with fall time approximating to that of the field produced by an approaching leader.

A critical test requires not only measurement of the respective probabilities of striking to active and passive rods, but also information on the time during the impulse at which the strike occurs.

The classical method to test an ESEAT in a laboratory is to use the French Standard NFC 17-102 (09/2011) [11] which describes the testing condition and evaluation criteria for ESEAT. Electrical, mechanical, environmental as well as electromagnetic compatibility requirements are fully explained in the standard. The effectiveness of the ESEAT is assessed by way of comparing, in a high voltage laboratory, the emission time of the ascending tracer, which it emits with the one a reference single rod air terminal (SRAT) emits. To achieve this, the SRAT and the ESEAT are assessed one after the other under the same electrical and geometrical conditions during laboratory tests that simulate natural discharge capturing start-up conditions (ascending positive tracer). The natural wave that exists before a lightning strike has consequences on the forming conditions of the corona and the pre-existing space-charge. It is therefore necessary to simulate it by applying a direct current that creates electric fields between the plate and the ground ranging between 20 kV/m and 25 kV/m. The impulse field may be simulated by a switching impulse whith fall time ranging between 100 µs to 1000 µs. The waveform slope when the upward leader initiates should be between 2.10^8 and 2.10^9 V/m/s. The impulse field is preferably simulated with a 250/2500 µs shaped operational wave as per CEI 60060-1.

The chosen criterion in the standard for assessing the effectiveness of ESEAT is its ability to repeatedly emit an ascending tracer before SRAT placed under the same conditions. For each usable impact on the SRAT and on the ESEAT, one measures the value of the emission time of the upward leader. Based on the measurements of the ascending tracer's emission times taken from SRAT and ESEAT, the average emission times $T_{moySRAT}$ and $T_{moyESEAT}$ are calculated.

The standard deviations of the two distributions are also calculated (σ_{SRAT} and σ_{ESEAT}).

While using the reference wave shape (fall time = 650 μs), one deduces the emission times related to the reference curve $T_{moy'SRAT}$ and $T_{moy'ESEAT}$ used for calculating the early streamer emission $\Delta T(\mu s) = T_{moy'SRAT} - T_{moy'ESEAT}$.

The tested lightning conductor of an ESEAT is in accordance with the French Standard if both of the following conditions are met:

$T_{moy'ESEAT} < T_{moy'SRAT}$ and $\sigma_{ESEAT} < 0.8.\sigma_{SRAT}$.

ΔT shall range between 10 μs and 60 μs. It is assumed that the earlier streamer "elongates" the height of ESEAT and by this manner the attractive area of active devices increases by the distance of ΔL.

Other experiments are available in open literature which enable us to prove the effectiveness of the ESE terminals in laboratory. As an example, it is possible to directly test the ESE terminal in comparison with a traditional Franklin rod. If the geometrical configuration is the same, then the discharges must be systematically initiated on the ESE terminal. These conditions were satisfied in experiments performed by Bouquegneau [6] in which the numbers of strikes were measured, out of two groups of 100 shocks, to an active and a passive rod mounted l.00 m and 2.00 m apart and symmetrically placed in relation to an upper rod electrode suspended vertically above the mid-point of the line joining the bases of the two rods. An impulse voltage (1.2/50 μs) was applied to the upper rod. The active rod was excited by a steady 25 kV voltage applied from a separate supply; active corona is assumed to have been set up. The results showed no significant difference between the rates of striking with regard to the active and passive rods. The tests, however, could not be regarded as conclusive, since the impulse voltage to the upper rod was too fast to simulate the effects of the leader descent and no preceding steady electric field was provided. Generally, similar tests on commercial devices have been carried out more recently by Grzybowski et al [7] with similar results.

Finally, we can find some data in literature where ESEAT are tested outside under operating conditions. Some publications may show failures in ESEAT functioning [3, 5, 9, 12]. As an example, many cases of ESEAT and radioactive terminal failures in Malaysia were recorded in recent years [5]. The failures in Kuala Lumpur were often detected on buildings higher than 60 m. In another field study, Hartono [12] has documented many instances of lightning strikes to structures in Malaysia and Singapore, which bypassed ESEAT installed on them, and struck parts with the structures within the zones of protection claimed for the terminals.

The aim of this present paper is to give a novel method to prove the effectiveness of ESEAT versus a traditional Franklin rod in a laboratory with a direct comparison of these two devices. Unlike previous work [6-7], the geometrical and electrical configurations are identical to that of the French Standard. Before experimental tests, a theoretical analysis of an active rod is presented.

3 THEORETICAL ANALYSIS OF AN ACTIVE ROD

3.1 THEORETICAL BASIS OF THE MODEL UNDER CONSIDERATION

As far as the theoretical aspect is concerned, the first stage can be correctly described by the quasi-electrostatic field equations while the development of the main stage phenomena requires an electrodynamic description. Due to the existence of the first stage one can formulate a relatively simple mathematical model on the basis of which various active ESEAT designs can be sought.

In this part, a model being a modification of the conventional solution is considered. The modification consists in the magnetic assistance of discharge development. The theoretical analysis presented below shows that it is possible to enhance lightning protection effectiveness. Franklin's idea of lightning protection is still preserved and under the same conditions the probability of lightning stroke occurrence and localization may increase.

It is shown that the principal physical mechanism producing an active rod action is the possibility of a spontaneous initiation (once the spark gap is triggered) of a transient state inducing (due to the character of voltage oscillation – a change of the voltage sign). The electric field intensity induced in an active rod is twice as powerful as the steady-state field generated when a conventional, non-active lightning rod is used [13]. This fact basically constitutes the main physical premise for the higher effectiveness of active rods.

The equivalent circuit diagram under consideration (Figure 1) represents our active rod design.

The following quantities are specified in the equivalent circuit diagram:

C_a: an active rod partial capacitance connected with the charge accumulated on the cloud's surface,

C_0: an active rod partial capacitance connected with the charge accumulated on the earth's surface,

C_i : the design capacitance of the rod's spark gap,

L, R: the inductance of the rod's internal coil, the total resistance of the rod and the earth electrode,

U_a: the cloud's atmospheric charge voltage relative to the earth,

u: the voltage between the rod's surface and the earth's surface,

i: transient-state current generated by the shorting of a spark gap with capacitance C_i,

Q: the total charge accumulated on the rod's surface,

E_0: the intensity of the external induction field.

C: the rod's total capacitance $C=C_a+C_0$ with neglected spark gap capacitance $C_i<<C$ as much smaller,

u_0: the rod's voltage relative to the earth prior to spark gap shorting in the static state.

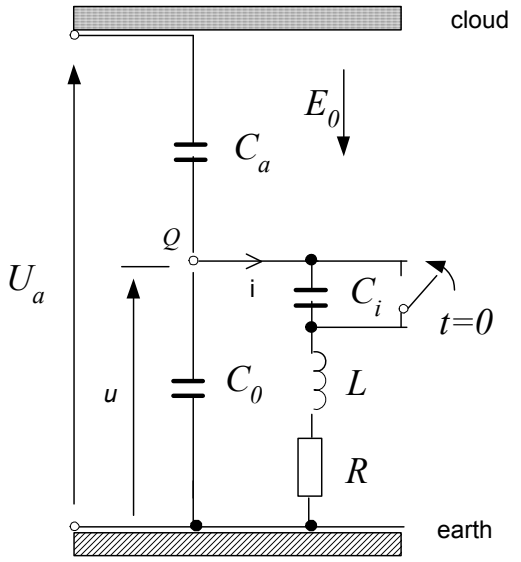

Figure 1. Equivalent circuit diagram of active rod.

3.2 FORMULATION AND SOLUTION OF INITIAL EQUATIONS

First the static state of charge with initial conditions i=0, $u=u_0$ Q=0 for t<0 prior to spark gap shorting was analyzed. Assuming a zero initial charge, from the total charge conservation law one gets the following equation:

$$(u_0 - U_a)C_a + (C_0 + C_i)u_0 = 0 \tag{1}$$

Hence:

$$u_0 = \frac{C_a}{C_a + C_0 + C_i}U_a \approx \frac{C_a}{C}U_a \tag{2}$$

Where:

C - is the rod's total capacitance $C=C_a+C_0$ with neglected spark gap capacitance $C_i<<C$ as much smaller,

u_0 - the rod's voltage relative to the earth prior to spark gap shorting in the static state.

After spark gap shorting at t≥0 a transient state occurs, which is defined by the charge and voltage balance equations:

$$C_a(u - U_a) + C_0 u + \int_0^t i\,dt = 0 \tag{3}$$

$$u = L\frac{di}{dt} + R\,i \tag{4}$$

The following relation is derived from equation (3) after differentiation:

$$i = -C\frac{du}{dt} \tag{5}$$

from which after substitution into equation (4) one gets this differential equation:

$$LC\frac{d^2u}{dt^2} + RC\frac{du}{dt} + u = 0 \tag{6}$$

with initial conditions $u(0)=u_0$, i(0)=0

After substituting $u=Ae^{pt}$ the characteristic equation:

$$LCp^2 + RCp + 1 = 0 \tag{7}$$

has complex roots $p=-\alpha+j\omega$ when

and the solution of equation (6) has this oscillatory form

$$u = u_0\,e^{-\alpha t}\left(\cos\omega t + \frac{\alpha}{\omega}\sin\omega t\right) = u_0 e^{-\alpha t}\,\frac{\cos(\omega t - \varphi)}{\cos\varphi} \tag{8}$$

with the following auxiliary denotations successively introduced:

attenuation coefficient $\alpha = R/2L$,

oscillation pulsation $\omega = \sqrt{1/LC - \alpha^2}$,

phase angle $\varphi = arctg\frac{\alpha}{\omega}$

For the conventional rod in which L=0, $u=u_0\exp(-t/RC)\rightarrow 0$ there is a direct connection of the rod with the earth and voltage u is permanently equal to zero.

From the solution for voltage one can determine the waveform of the charge accumulated on the rod's surface. From the balance equation:

$$Q = C_a(u - U_a) + C_0\,u = -C_a U_a + C\,u \tag{10}$$

taking into account (2) and (8) one gets the relation

$$Q = -C_a U_a\left[1 - e^{-\alpha t}\,\frac{\cos(\omega t - \varphi)}{\cos\varphi}\right] \tag{11}$$

$$\frac{Q}{Q_0} = 1 - e^{-\alpha t}\,\frac{\cos(\omega t - \varphi)}{\cos\varphi} \tag{12}$$

where $Q_0=-C_a\,U_a$ stands for the charge accumulated in the steady state, which is equal to the charge of the conventional rod (at u=0).

It is apparent that the right side of equation (12) assumes the highest value for $\omega t_m=\pi$, which may be expressed by the formula:

$$k_m = \max_t\left[1 - e^{-\alpha t}\,\frac{(\cos\omega t - \varphi)}{\cos\varphi}\right] = 1 + e^{-\frac{\alpha}{\omega}\pi} \tag{13}$$

Hence at $\alpha \approx 0$, $k_m \approx 2$.

One can also check through direct calculations whether the derivative of function (12) is equal to zero:

$$\frac{d}{dt}\left[1 - e^{-\alpha t}\,\frac{\cos(\omega t - \varphi)}{\cos\varphi}\right] = 0 \tag{14}$$

when $\omega t=\pi$, which validates formula (13).

Expressing the exponent in formula (13) by parameters R, L, C, one gets the relation:

$$\frac{\alpha}{\omega}\pi = \frac{1}{\sqrt{4k_Q^2 - 1}} \tag{15}$$

where quality factor k_Q and characteristic resistance ρ are defined by the formulas:

$$k_Q = \frac{\rho}{R} \tag{16}$$

$$\rho = \sqrt{\frac{L}{C}} \tag{17}$$

Figure 2 shows a diagram of peak value k_m (expressed by formula (13)) as a function of system quality factor, calculated for a range of $0.5 < k_Q < 100$.

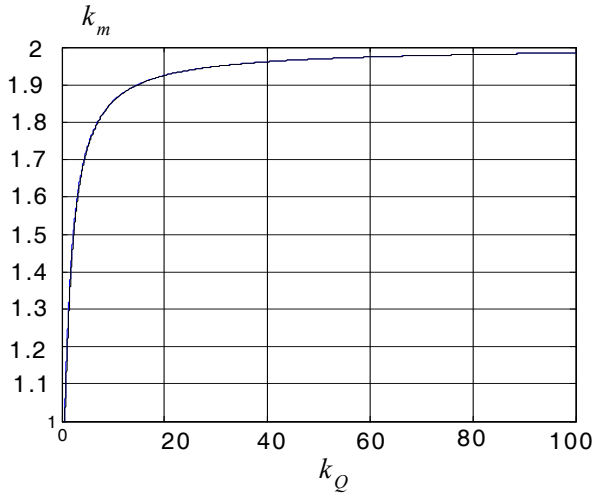

Figure 2. Peak value k_m versus quality factor k_Q.

In practice, the system quality factor is higher than 15 and so the peak value of active rod charge is nearly twice as high as that of the charge of the conventional Franklin rod with the same C_0 and C_a.

3.3 DETERMINATION OF FIELD DISTRIBUTION

In order to qualitatively evaluate the discharge phenomenon, a more detailed analysis of the field distribution is needed. For this purpose a spherical rod with radius r_0, was selected and placed in a uniform primary field with intensity E_0. The other adopted symbols are shown in Figure 3.

In the initial situation, corresponding to the initial state, the conducting sphere is insulated and its initial charge is equal to zero: Q(0)=0.

According to the known theory [13], under the assumptions made the sought field potential distribution can be determined as a superposition of the external field and the point dipole field and it is expressed by the formula:

$$V = r\cos\Theta E_0 - \frac{p\, r\cos\Theta}{4\pi\,\varepsilon\; r^3} + const;\;\; r \geq r_0 \quad \varepsilon = \varepsilon_0 \tag{18}$$

where: p- the electric moment of the point dipole, ε_0- the permittivity of free space.

The potential on the surface of the sphere with $r=r_0$ is expressed by the formula:

$$V_0 = r_0\;\cos\Theta E_0 - \frac{p\, r_0\cos\Theta}{4\pi\varepsilon\, r_0^{\,3}} + const \tag{19}.$$

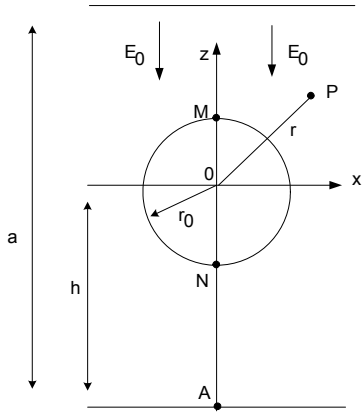

Figure 3. Rod in form of conducting sphere in external field E_0.

Assuming dipole moment:

$$p = 4\pi\varepsilon\, r_0^3 E_0 \tag{20}$$

one gets sphere surface equipotentiality V_0=const.

Fixing the potential in point A on the earth's surface, equal to zero $V_A=0$ for r=h, $\Theta=\pi$ in formula (18) one gets:

$$0 = (-h)E_0 - \frac{p(-h)}{4\pi\varepsilon(h)^3} + V_0 \tag{21}$$

and taking into account (20) one determines sphere potential V_0.

$$V_0 = hE_0\left(1 - \frac{r_0^3}{h^3}\right) \approx hE_0 \tag{22}$$

where the approximation can be used at $r_0 << h$.

Taking the above relations (18, 20, 22) into account one gets for $r \geq r0$ the potential expressed by the formula:

$$V = (h + r\cos\Theta)\, E_0\left(1 - \frac{r_0^3}{r^3}\right) + V_0 \tag{23}$$

The highest field intensity in this state occurs in points M, N on the sphere's surface and it can be calculated as the derivative of potential (23)

$$E_{M,N} = -\frac{\partial V}{\partial r} = -3E_0\cos\Theta, \quad M(r = r_0, \Theta = 0), N(r = r_0, \Theta = \pi) \tag{24}$$

Under the assumption that the sphere's surface is not neutral, but charged with charge Q the distributions of potential and field intensity in points M and N are expressed by the respective relations:

$$V = (h + r\cos\Theta)E_0\left(1 - \frac{r_0^3}{r^3}\right) + V_0 + \frac{Q}{4\pi\varepsilon}\left(\frac{1}{r} - \frac{1}{h}\right) \tag{25}$$

$$E_M = -3E_0 + \frac{Q}{4\pi\varepsilon\, r_0^2} \tag{26}$$

$$E_N = -3E_0 - \frac{Q}{4\pi\varepsilon\, r_0^2} \tag{27}$$

It follows from the above formulas that at negative charge $Q<0$ and $E_0>0$ field intensity reaches a higher absolute value in the upper point M than in the lower point N. The value of charge Q which will flow to and accumulate on the surface of the sphere depends on the potential induction on the former.

Let us consider two cases:

a) According to solution (8), for the active rod in a transient state the potential of the sphere's surface may assume an instantaneous value (change polarization) reverse to the static-state potential relative to the earth: V= -V_0.

b) In the case of the conventional rod, the sphere surface potential for the direct connection with the earth assumes the value of zero: V=0.

Hence from equations (23) and (22 in case a) the charge is expressed by the formula:

$$Q_a = -2V_0 4\pi\varepsilon\left(\frac{1}{r_0}-\frac{1}{h}\right)^{-1} = -8\pi\varepsilon E_0 r_0 h\left(1+\frac{r_0}{h}+\frac{r_0^2}{h^2}\right) \quad (28)$$

and in case b)

$$Q_b = -V_0 4\pi\varepsilon\left(\frac{1}{r_0}-\frac{1}{h}\right)^{-1} = -4\pi\varepsilon E_0 r_0 h\left(1+\frac{r_0}{h}+\frac{r_0^2}{h^2}\right) \quad (29)$$

The peak values of field intensity on the surface of the active rod and on that of the conventional rod are expressed by the respective formulas:

$$E_{Ma} = -3E_0 + \frac{Q_a}{4\pi\varepsilon r_0^2} = -\left[3+2\left(\frac{h}{r_0}+1+\frac{r_0}{h}\right)\right]E_0 \quad (30)$$

$$E_{Mb} = -3E_0 + \frac{Q_b}{4\pi\varepsilon r_0^2} = -\left[3+\left(\frac{h}{r_0}+1+\frac{r_0}{h}\right)\right]E_0 \quad (31)$$

The degree of field intensity concentration (relative to the primary induction field value) on the surface of the active rod and on that of the conventional rod can be calculated from the respective formulas:

$$k_{Ea} = \left|\frac{E_{ma}}{E_0}\right| = 3+2\left(\frac{h}{r_0}+1+\frac{r_0}{h}\right) \quad (32)$$

$$k_{Eb} = \left|\frac{E_{mb}}{E_0}\right| = 3+\left(\frac{h}{r_0}+1+\frac{r_0}{h}\right) \quad (33)$$

In a more general case (as regards the shape of the rod's surface), it follows from the problem linearity that field intensity in point M of maximum concentration consists of two components: a component proportional to primary field intensity E_0 and a component proportional to the largest charge accumulated on the rod's surface $Q=k_m.Q_0$ (formulas (12) and (13))

Hence ultimately the concentration coefficient (32), (33) assumes this form:

$$k_E = \frac{E_M}{E_0} = k_{E1} + k_m k_{E2} \quad (34)$$

Where:

$k_{E1}=\beta_E$ represents the static-state field concentration coefficient when the rod is disconnected (insulated) from the earth (Q=0),

$k_{E2}=C_a.a.\beta_Q$ represents the steady-state field concentration coefficient when the rod is permanently connected to the earth ($u=0$),

k_m stands for the transient-state peak value coefficient expressed by formula (13).

Assuming approximately r_0=0.1 m, h=10 m one calculates concentration coefficients kE_a=205, kE_b=104 from (32) and (33). The nearly twice higher field concentration in the case of the active rod is a factor increasing its operating effectiveness.

Assuming air strength E_w=30 kV/cm one gets external field E_0=30/205≈15 kV/m, which may cause the development of a full discharge. At cloud altitude a=0.5 km, the cloud voltage relative to the earth triggers discharge $U_a=E_0.a$=7.5 MV.

In the case of the spherical rod the concentration coefficients (34) amount to kE_1=3, kE_2=101, k_m=2, k_E=205.

The above coefficient values depend on the geometric shape of the rod and may be much higher at a smaller radius of curvature of the rod's surface.

The theoretical analysis carried out in this paper shows that the active rod is more effective than the conventional Franklin lightning rod. Physically, the achieved effect of increased field intensity concentration ($k_m\approx2$) stems from the reversal of the voltage sign during transient-state oscillations. As a result, the rod's potential becomes lower than the earth's potential whereby the active rod is overcharged with a nearly twice as large charge as that of the conventional rod. The induction element plays a significant role in the development of this phenomenon. In energy terms, higher instantaneous electric field energy results from the addition of the magnetic field energy accumulated in the induction element. The increase in field concentration causes increased air ionization in the neighborhoods of the rod, creating conditions conducive to the formation of a streamer and consequently, to total discharge. On the basis of the physical premises active rods can increase lightning protection effectiveness.

4 EXPERIMENTAL SET-UP AND PROTOCOL

4.1 HV SET-UP

The experiments were carried out with two ESEAT manufactured by the Piorteh Company at the High Voltage laboratory of the University of Pau in France. The cloud was simulated by a L=2.35 m diameter metal plate, to which the high negative voltages were applied, suspended above the air terminations to be tested, which were mounted on the laboratory floor (Figure 4).

The distance between the metal plate and the grounded laboratory floor is H=2.20 m. The air gap length between the plate and the lightning protection system is d=1.10 m. Then the distance between the two ESEAT is fixed to d_1=1.00 m (see part 4.2).

During the tests, a negative DC voltage of -49.5 kV was applied to the high voltage electrode. This value is necessary to simulate the natural atmospheric electric field that exists before a lightning strike by applying a direct current that creates an electric field between the metal plate and the ground of 22.5 kV/m. The air gap was triggered with the help of a conventional Marx generator of maximum peak voltage 1 MV and 350 µs fall-time. Thus the metal plate is energized by the apparatuses presented in Figure 5.

These geometrical and electrical arrangements are completely in accordance with the experimental set-up and conditions specified in the latest French Standard NFC 17-102 (09/2011) prevailing at the time of testing.

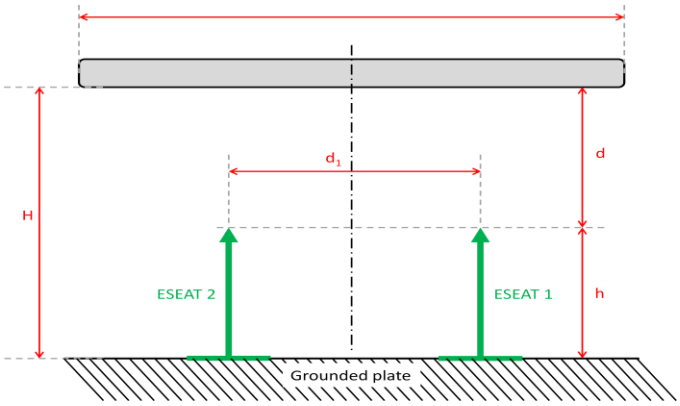

Figure 4. Dimensions of the experimental set-up.

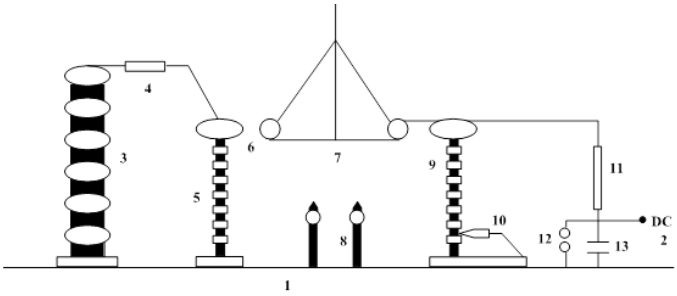

Figure. 5. Apparatuses used in the experiment.

1: Grounded plate
2: High voltage DC power supply (-100 kV)
3: Marx generator
4: Resistance in series with the generator: 70 kΩ
5: Adjustment waveform capacitor: 666 pF, 700 kV
6: Insulation gap: insulate up to 60 kV the Marx generator from the continuous voltage (-49.5 kV)
7: Metal plate
8: ESEAT under test
9: Capacitive divider (40 pF, 1MV, ratio 1/24.6)
10: North Star commercial probe (1/1000)
11: Load resistor (100 MΩ)
12: Security gap (set-up: 60 kV)
13: 1nF capacitor (integrating circuit of the impulse)

In all the experiments, initiation of corona at the terminations was detected by photomultiplier observation of the light emission. Time to breakdown, between plate and rod, was found from the potential divider observation of the collapse of voltage across the gap.

The measurement of the voltage delivered by the Marx generator is achieved by means of a capacitive voltage divider (40 pF, 1 MV) and a commercial North Star voltage probe.

The acquisition of electrical signals such as the waveform and the voltage signal output from the photomultiplier is performed with the use of a Tektronix 3054 digital oscilloscope (500 MHz/5 GS.s-1).

Meteorological conditions during the tests were recorded as follows:

Temperature: $20\ °C < T < 22\ °C$
Humidity: $46\% < \delta < 52\%$
Pressure: 0.1 MPa (1019 mbar)

It can be assumed that the climatic conditions in the laboratory were nearly the same during the tests.

The first tests were carried out in accordance with French Standard NF C 17-102. The conclusion is that the upward leader initiation advance time of the PiX3-60 is superior to 60 µs. Besides the experimental results obtained satisfy the following conditions:

- $T_{moy'ESEAT} < T_{moy'SRAT}$
- $T_{moy'ESEAT} - T_{moy'SRAT} > 10\ \mu s$
- $\sigma_{ESEAT} < 0.8\ \sigma_{SRAT}$

The PiX3-60 early streamer emission air terminal appeared to be intact and in good condition after the test as only very minor stains were observed on its main and auxiliary electrodes.

4.2 SRAT AND ESEAT RELATIVE LOCATION

Before experiments on both devices are undertaken, it is important to find the laboratory locations for which the two ESEAT are placed in the same electromagnetic environment. The electric devices of big size (Marx generator, capacitor or capacitive divider in Figure 5) must not influence the electromagnetic field distribution in the vicinity of the two ESEAT. That is why electrostatic simulations are needed. They are aimed at determining the minimal distance d_1 between the two ESEAT and so at finding the best configuration for the location of them. CST EM Studio 3-D electrostatic solver [14] includes solver modules ideally suited to the analysis of static and low frequency devices.

Experimental conditions as outlined above were simulated, with Figure 6 presenting 2-D and 3-D views of the electric field distribution for negative polarity. The applied voltage is -500 kV and the distance d_1 between the two ESEAT is 1.00 m.

Figure 7 shows the electric field distribution along the vertical central axis from the tip to the cloud of the arrangement. The tip of the rod corresponds to the origin d=0 m while the plate is located at d=1.10 m. The result with a single ESEAT located above the cloud is also given in order to compare the electric field distribution. The results show that the electric field generated in the immediate vicinity of the rod is very strong i.e., approximately 35 kV/cm. Thereafter, it decreases exponentially towards the metal plate, where it is only 4 kV/cm. Most importantly is the comparison between the electric field distributions provided by the three curves. The results are quite similar. That is why we can conclude that the electromagnetic environment, due to all the apparatuses does not modify the future experimental results. This result is valid from a distance d_1=0.80 m. But during the tests, the distance d_1 is always chosen to be 1.00 m.

Figure 8 presents also the horizontal electric field distribution between the two tips of the ESEAT spaced by a 1.00 m distance. The origin d=0 m corresponds to the tip of the rod of the ESEAT1 while d=1.00 m corresponds to the tip of the other ESEAT2. A good symmetry is observed along this horizontal axis between the two ESAT when they are spaced by a 1.00 m distance.

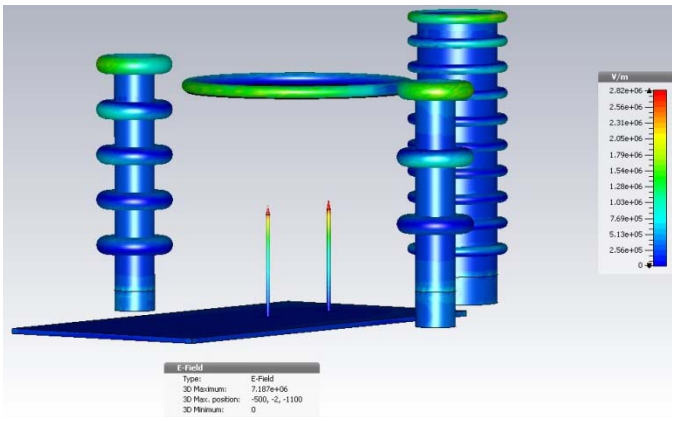

(a)

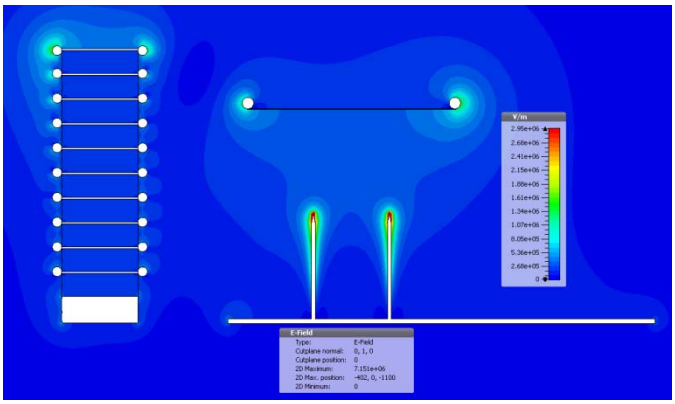

(b)

Figure 6. Electric field distribution obtained with CST software in negative polarity for an applied voltage of -500 kV and a distance d_1=1 m
(a) 3-D view and (b) 2-D representation.

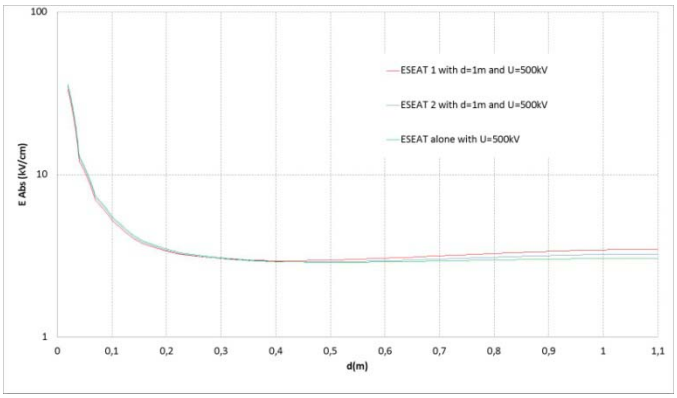

Figure 7. Electric field distribution for a single ESEAT and for two ESEAT located at a distance d_1=1.00 m (V= -500 kV).

Figure 8 presents also the horizontal electric field distribution between the two tips of the ESEAT spaced by a 1.00 m distance. The origin d=0 m corresponds to the tip of the rod of the ESEAT1 while d=1.00 m corresponds to the tip of the other ESEAT2. A good symmetry is observed along this horizontal axis between the two ESAT when they are spaced by a 1.00 m distance.

4.3 EXPERIMENTAL PROROCOL

For each configuration, the first 30 usable impacts were recorded. The delay between two impacts was 2 minutes.

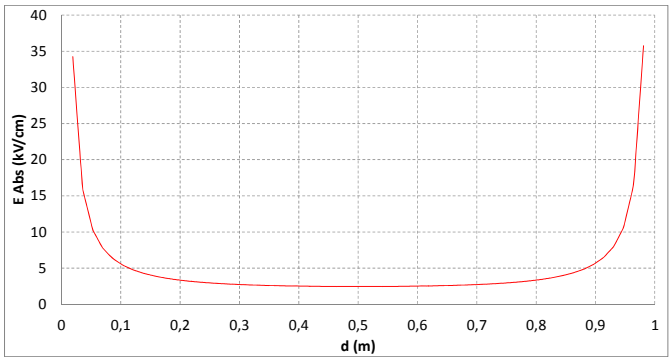

Figure 8. Horizontal electric field distribution between the two ESEAT spaced by a 1.00 m distance.

The first step of the tests consisted in finding an experimental configuration in which the strikes are observed, almost alternately on one or the other of the two ESEAT positioned under the metal plate. The first 30 shocks were used to determine the U_{50} voltage through the "up and down" method. The following 30 shocks are done for a voltage slightly above this value. Two ESEAT (PIX3-60 manufactured by the Piorteh Company) are tested and they are previously shorted to make them inactive. We estimate that this is the best solution to form the Franklin terminals from ESEAT after grounding the tips of ESEAT. Such procedure ensured that the shape of ESEAT and Franklin terminals was identical. We note the number of the shock, the voltage value at the breakdown time of the gap (U_b), and the time of breakdown (T_b) which elapsed between the application of the voltage waveform and the dielectric breakdown. Finally, we note especially the ESEAT on which the discharge was initiated.

In a second step, the ESEAT1 is activated while ESEAT2 remains shorted. We note, again, for a series of 30 shocks, the number of the shock, the voltage value at the time of dielectric breakdown of the gap (U_b), the time of breakdown (T_b) as elapsed between the application of wave voltage and dielectric breakdown and of course always the ESEAT on which discharge was initiated. The average value of T_b obtained when the lightning protection system was inactive is then compared to that obtained when the lightning ESEAT1 is active.

5 EXPERIMENTAL TESTS AND RESULTS

During the first experiments the two ESEAT are shorted (Figure 10). They can be considered as inactive and equivalent to a traditional Franklin rod. In this configuration, the U_{50} voltage is 479.1 kV with an average time to breakdown of 285 µs. During experiments, initiation of corona at the terminations was detected by photomultiplier observation of the light emission. Figure 9 presents the electrical activity near the tip of an ESEAT when an impulse voltage is applied. There is no breakdown here but we can note that the corona initiation is effective during the first 300 µs and it promotes the breakdown when the electric field reaches its maximum amplitude.

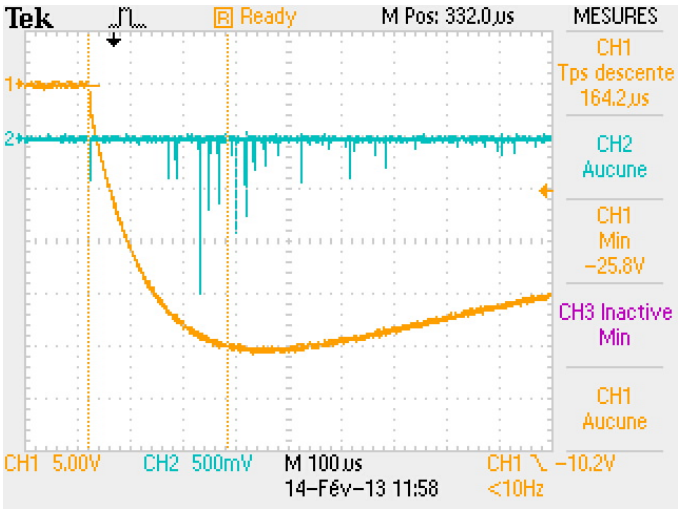

Figure 9. Initiation of corona near the ESEAT terminations detected by means of a photomultiplier (CH1: voltage waveform with 1 V=18 kV and CH2: signal output from the photomultiplier).

Then, with a slight increase of the voltage delivered by the Marx generator, test results show a complete homogeneous distribution of breakdowns: 15 breakdowns were recorded on each ESEAT unit. The average breakdown voltage is 490.9 kV with an average time to breakdown of 299 µs and a standard deviation of 62 µs.

Figure 10. ESEAT1 and ESEAT2 are shorted during the first experiment (adhesive thin sheets of copper are used on both devices).

When the ESEAT1 is activated while ESEAT2 remains shorted (Figure 11), the breakdown distribution is completely changed: all discharges (30 shocks) are now initiated from the active lightning rod i.e. the ESEAT1.

We also note that the average time to breakdown in this case (241 µs) is below the average time to breakdown when both ESEAT are inactive (299 µs). In addition, the standard deviation for the active ESEAT2 (43 µs) is less than 80% of the deviation obtained when both ESEAT are inactive.

Figure 11. ESEAT1 is active and ESEAT2 is shorted during the second experiment (thin adhesive sheets of copper are used only on one device).

Similar results were obtained by reversing the two EEAT (the ESEAT1 becomes active and the ESEAT2 inactive).

This novel experimental technique demonstrates clearly the effectiveness of the Pix3-60 ESEAT manufactured by Piorteh Company in the High Voltage laboratory of the University of Pau.

6 CONCLUSIONS

In this paper, the theoretical analysis carried out shows that the active rod is more effective than the conventional Franklin lightning rod. The peak value of active rod charge is almost twice as high as that of the charge of the conventional Franklin rod and the induction element plays a significant role in the development of this phenomenon.

A novel method of experimental test evaluation in the High Voltage laboratory of the University of Pau in France confirms the theoretical conclusions. Unlike the NFC 17-102 French Standard (09/2011), where the tests are carried out alternately on an inactive device and then on an ESEAT, our method is to test both devices simultaneously. In our experimental configuration, all discharges are observed on the active device.

In order to fully evaluate the protection effectiveness, real-scale tests need to be carried out. As an example, the photograph presented in Figure 12 points out the effectiveness of the lightning protection devices manufactured by Piorteh Company in nature during a storm at the Millau Viaduct in France (August 6, 2013). On this picture, the effectiveness of ESEAT from Piorteh Company is clearly visible.

Figure 12. Photograph of lighning strikes on Piorteh's ESEAT protecting the Millau Viaduct in France (06/08/2013).

REFERENCES

[1] N.L, Allen, K.J. Cornick, D.C. Faircloth and C.M. Kouzis, "Tests of the early streamer emission principle for protection against lightning", IEE Proc. Sci. Measurement and Technology, DOI:10.1049/ip-smt:19982209, 1998.

[2] V. Rakov and A. Martin, *Lightning: Physics and Effects*, Cambridge University Press, ISBN 978052035415, 2003.

[3] W. Rison, "Experimental validation of conventional and non-conventional lightning protection systems", IEEE Power Engineering Society General Meeting, Vol. 4, DOI:10.1109/PES.2003.1270959 ISBN: 0-7803-7989-6, 2003.

[4] S. A. Amar and G. Berger, "A modified version of the rolling sphere method ", IEEE Trans. Dielectr. Electr. Insul., Vol. 16, No. 3, pp. 718-725, 2009.

[5] K.L. Chrzan and Z.A. Hartono, "Inefficacy of radioactive terminals and early streamer emission terminals", XIIIth International Sympos. High Voltage Engineering, ISBN 90-77017-79-8, p. 86, 2003.

[6] C. Bouquegneau, "Laboratory tests on some radioactive and corona lightning rods", 18th Int'l. Conf. Lightning protection, Munich, Germany, pp. 37-45, 1985.

[7] S. Grzybowski, A.L. Libby, J.R. Gumley and S.J. Gumley, "Comparative testing of ionizing and non-ionizing air terminals", 10th Int'l. Sympos. High voltage engineering, Montreal, Vol. 5, pp. 331-334, 1997.

[8] Z. Flisowski and P. Korycki, "Advertised and actual effectiveness of lightning rods with early streamer emission (ESE)", Przegląd Elektrotechniczny, No. 11, 282, 1998 (in Polish).

[9] Z.A. Hartono, I. Robiah and M. Darveniza, "A database of lightning damage caused by bypasses of air terminals on buildings in Kuala Lumpur, Malaysia", 6th Int'l. Sympos. Lightning Protection, Santos, Brazil, pp. 211-216, 2001.

[10] M. Uman, *The Lightning Discharge*, Academic Press, Chapter 3, Orlando, 1987.

[11] French Standard NFC 17-102. "Protection against lightning. Early streamer emission air terminals", 2011.

[12] Z. Hartono and I. Robiah, "The Collection Surface Concept as a Reliable Method for Predicting the Lightning Strike Location", 25th Int'l. Conf. Lightning Protection, pp. 328-333, 2000.

[13] P. Moon and D. E. Spencer, *Field Theory for Engineers*, Princeton, Toronto, London, New York, 1961.

[14] Computer Simulation Technology (CST), https://www.cst.com/, last time accessed in November 2013

Laurent Pécastaing received the Ph.D. degree and the Research Directorship Habilitation in electrical engineering from the Université de Pau et des Pays de l'Adour, Pau, France, in 2001 and 2010, respectively.
He is currently a Lecturer with the Laboratoire SIAME, Université de Pau et des Pays de l'Adour. His research interests are focused on high-power microwave (HPM) sources, compact pulsed power devices, including pulse-forming lines or Marx generators, and ultrafast transient probes.

Antoine Silvestre de Ferron was born in Tarbes, France, in 1977. He received the Ph.D. degree in electrical engineering from the Université de Pau et des Pays de l'Adour (UPPA), Pau, France, in 2006. From 2006 to 2008, he was a Researcher with the Atomic Energy Comission (CEA), Le Barp, France – a French-government-funded technological research organization. He is currently an Engineer with the Laboratoire SIAME, UPPA.
His research interests include high pulsed power generation for military and civil applications and combined high-voltage transient probes.

Thierry Reess was born in Pau, France, in 1968. He received the M.Sc. degree in plasma physics from the University of Toulouse, France, in 1992 and the Ph.D. degree in electrical engineering from the University of Pau, France, in 1996. He is currently a lecturer with the Electrical Engineering team of the SIAME laboratory, University of Pau, France. His research interests include high power devices and electrical discharges in gases and liquids.